The Monte Carlo Method: Versatility Unbounded In A Dynamic Computing World
Chattanooga, Tennessee, April 17–21, 2005, on CD-ROM, American Nuclear Society, LaGrange Park, IL (2005)

DESIGN OF A MODERATOR ASSEMBLY DELIMITER FOR AN ABNS FOR BNCT

Joshua P. Sroka, Thomas E. Blue, Chenguang Li, Andrew E. Hawk and Nilendu Gupta
Department of Nuclear Engineering
The Ohio State University
650 Ackerman Road, Columbus Oh, 43202
sroka.5@osu.edu; blue.1@osu.edu; gupta.6@osu.edu

ABSTRACT

As part of an effort to design a moderator assembly for an Accelerator Based Neutron Source (ABNS) for Boron Neutron Capture Therapy (BNCT), we have implemented a modified version of the Zubal Phantom (a voxel-based head phantom that delineates detailed structures inside the brain) in MCNP. As the component of the moderator assembly that is closest to the patient, the shape and material of the delimiter is important to the quality of the neutron beam. Using our Zubal Phantom MCNP model, we have evaluated various moderator assembly delimiter designs. The evaluation was based on the calculation of a new neutron field assessment parameter (NFAP) that we developed to evaluate the complex dose distributions resulting from the mixed neutron and gamma-ray fields that arise in the head of an individual who is treated for a malignant brain tumor using BNCT. The modified Zubal phantom was used to calculate the absorbed doses of different structures in the brain as well as the tumor dose. The new NFAP is based on absorbed dose distributions for normal tissues/structures and tumor, and yields a score that accounts for the competing goals of sparing normal tissues and maximizing tumor dose. It was formulated by modifying a previously defined Objective Function, so that it is appropriate for BNCT. The resulting BNCT Objective Function (BOF) allows for the inclusion of tissue specific Relative Biological Effectiveness (RBE), and tissue specific dose tolerances and weights. In addition to assessing the effect of the delimiter on the BOF, the effect of the delimiter in reducing the whole body dose to the bone marrow was assessed using MCNP with a MIRD whole body phantom.

Key Words: BNCT, Accelerator Based Neutron Source

1 INTRODUCTION

This paper describes our efforts at The Ohio State University (OSU) to examine the design of a delimiter for an Accelerator Based Neutron Source (ABNS) for Boron Neutron Capture Therapy (BNCT). Our examination is based on calculations that were performed using the Monte Carlo code MCNP5. Two sets of calculations were performed. One set of calculations was performed to examine the effectiveness of the delimiter in shaping the radiation dose distribution within the patient's head. The other set of calculations was performed to examine the effectiveness of the delimiter in reducing the patient's whole body radiation dose. The former set of calculations was performed using the lattice entry feature of MCNP5 with a voxelized structure-based head phantom. The latter set of calculations was performed using MCNP5 with the adult male Medical Internal Radiation Dosimetry (MIRD) mathematical phantom developed by Cristy and Eckerman [1].

Both sets of calculations were performed for two modeled sources. One modeled source is based on a recent iteration of the OSU ABNS design. The other modeled source represents an

idealized neutron source (INS). The latter source was modeled to serve as an easily reproducible benchmark source, for the verification of our results by others and to help us recognize appropriate delimiter behavior in our calculations for the OSU ABNS design.

2 BACKGROUND

2.1 BNCT

Boron Neutron Capture Therapy is a surgically non-invasive, experimental radiation therapy developed for the treatment of malignant tumors, especially malignant tumors of the brain. BNCT was first proposed by Locher in 1936 [2]. In BNCT, a ^{10}B containing compound is introduced into a patient. The patient is then irradiated in an epithermal neutron field. Neutrons from this field thermalize as they pass through brain tissue resulting in a thermal neutron flux at and around a tumor site. The ^{10}B atoms, strongly absorb thermal neutrons in an (n,α) reaction and emit energetic α particles and ^{7}Li recoil nuclei that deposit their energy within approximately one cell diameter in the surrounding tissue.

In successful BNCT, tumor cells are destroyed while the surrounding healthy tissue remains, to as large an extent as possible, unharmed. There are three requirements that must be met in order to accomplish this. The first requirement is that a sufficiently large amount of ^{10}B must be delivered to the tumor cells. The second requirement is that the ^{10}B must be preferentially absorbed by the tumor cells, as opposed to healthy tissue. In addition, ^{10}B concentrations in the blood must be minimized to prevent excessive damage to the blood vessel walls. The third requirement is that a sufficiently large thermal neutron fluence must be delivered to the tumor site in a reasonable treatment time while respecting the tolerance of normal tissues to neutron dose. Fulfilling this last requirement with an ABNS has been the primary goal of the OSU ABNS design effort.

2.2 ABNS

Neutrons are produced in an ABNS by bombarding a target with charged particles. In the OSU-ABNS design, 2.5 MeV protons bombard a ^{7}Li target with currents on the order of a few tens of milliampers. The proton beam energy was chosen by Blue (1986) [3] based on visual inspection of the neutron production cross-section for the $^{7}Li(p,n)^{7}Be$ reaction.

Neutrons are produced in the ^{7}Li with an average energy of 400 keV. These neutrons are too energetic to be used for BNCT. Therefore a moderator assembly is placed, between the ^{7}Li target and the patient receiving a BNCT treatment, to reduce the energy of the neutrons to epithermal energies (1 eV –1 keV) [4]. The moderator assembly design has been under development at OSU for some time. The moderator assemblies that were modeled for this delimiter study are shown generically in Fig. 1, with a cross-section through the moderator assembly's central axis.

The moderator assembly's lateral profile is that of a right circular cylinder. However, it is in fact comprised of a number of objects of revolution: specifically a MgF_2 moderator, a CaF_2 reflector, and a CaF_2 delimiter. The lithium target and the target Heat Removal System (HRS) abut the moderator on its upstream side. The treatment port lies immediately downstream of the moderator and is formed by the hole in the center of the annular delimiter. The dimensions of the components of the moderator assembly are given in Fig. 1.

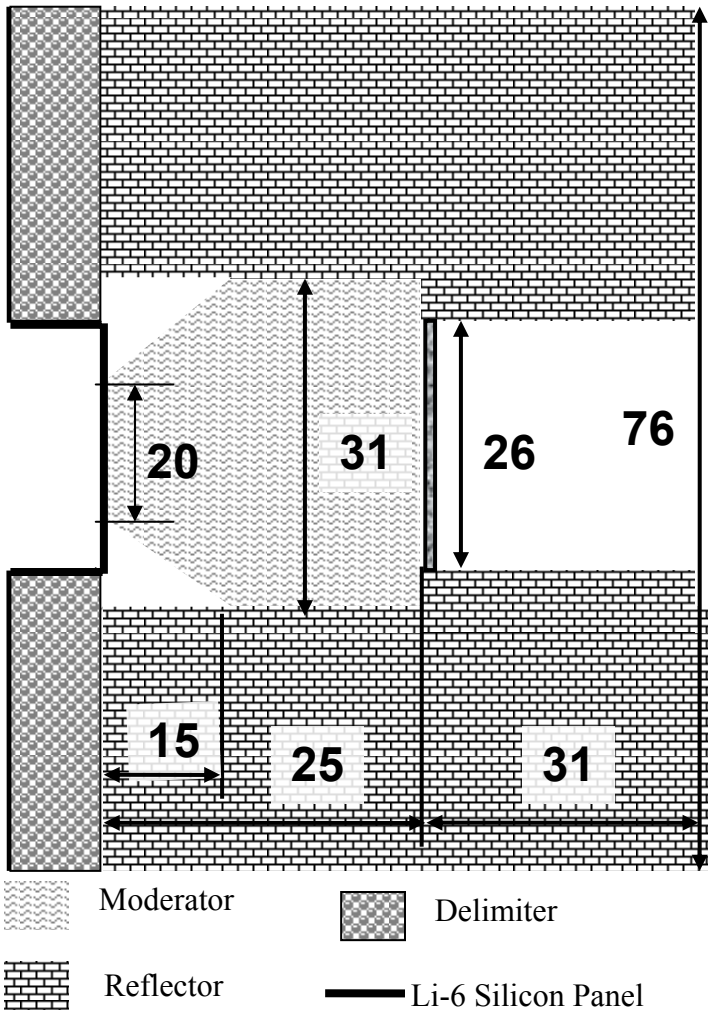

Figure 1. Geometry of the moderator assemblies (dimensions in cm)

The moderator assembly functions as follows. The proton beam enters the moderator assembly through the beam port the right hand side of Fig. 1. Beam protons strike the target causing the emission of neutrons. The neutrons emitted in the target pass through the moderator before irradiating the patient. In passing through the moderator, the average energy of neutrons is reduced to epithermal energies which are appropriate for BNCT. In moderating the neutrons to epithermal energies, the moderator provides some degree of protection to the patient with respect to fast neutron whole body dose. The moderator also shields the patient from gamma rays emitted in the target. Additional shielding is provided by the delimiter.

The intent of the delimiter is that it delimits the neutron field entering the patient. In so doing it shapes the radiation dose distribution within the patient's head and shields the patient's whole body from fast neutrons, epithermal neutrons and gamma rays. Additionally the downstream surface of the delimiter and the portion of the moderator assembly that forms the treatment port are lined with a thin layer of a lithiated silicon flex panel, which shields the patient form thermal neutrons.

The purpose of this paper is to examine the effectiveness of the delimiter in performing its dual roles of shaping the radiation dose distribution within the head and reducing the patients whole body radiation dose. In addition, the effect of the delimiter on the treatment time is examined. Of the many parameters that may be varied in the design of a delimiter, only two (the axial thickness of the delimiter and the diameter of the treatment port) are considered in this analysis.

2.3 Idealized Neutron Source

As mentioned in the Introduction, besides presenting calculations for moderator assemblies with delimiters of various thicknesses and treatment port diameters, this paper presents calculations for an Idealized Neutron Source (INS) of various diameters. The modeling of the INS is described below. The INS is a circular surface source that emits neutrons normally and uniformly from its front surface. The source has a 1/E neutron energy spectrum from 4×10^{-7} MeV to 0.33 MeV. The probability density function (PDF) for this spectrum is:

$$f(E) = \begin{cases} \dfrac{1}{E \ln(0.33/4\times10^{-7})}, 4\times10^{-7} \le E \le 0.33 MeV \\ 0, otherwise \end{cases} . \quad (1)$$

This energy spectrum is close to that for neutrons from the beam port of the OSU ABNS design. Since the photon absorbed doses in BNCT are a consequence of primarily (n, γ) reaction in the body tissues, a no primary photon source is not modeled in these calculations.

3 PATIENT PHANTOMS

We used two different phantoms for our studies. For the purposes of calculating the effectiveness of the delimiter in shaping the radiation dose distribution within the patient's head, we used the Zubal phantom. Hereafter such calculations will be referred to simply as Zubal phantom calculations. For the purposes of calculating the effectiveness of the delimiter in reducing the patient's whole body dose we used the MIRD phantom. Hereafter, such calculations will be referred to simply as MIRD phantom calculations. It should be noted that the calculations with the Zubal phantom include the torso and upper extremities of the MIRD phantom. The Zubal and MIRD phantoms are described below.

3.1 Zubal Phantom

The original Zubal phantom is a 3-D model of a head that was created from MRI images of a healthy human male that delineates phantom structures [Zubal et al.(1994)] [5]. In order to calculate the dose to tumor, we inserted a spherical tumor with a 1cm diameter within the phantom at 6cm depth, as measured from the inner surface of the skull along the beam centerline. Also, as described in Evans et al. (2001) [6], the phantom was compressed into an 85×109×120 one-byte array and translated into lattice format for entry into MCNP. Figure 2 shows a transverse cross-section from the head of the Zubal Phantom, for a slice without tumor.

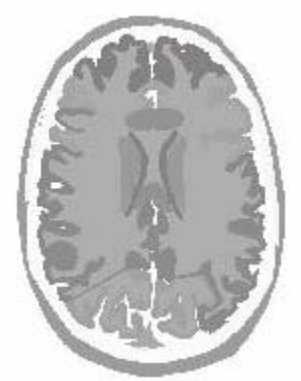

Figure 2. A transverse cross-section from the head of the Zubal Phantom as viewed with ImagJ

3.2 MIRD Phantom

The mathematical patient phantom used in the shielding calculations was the adult male phantom developed by Cristy and Eckerman (1987) [1]. The Cristy/Eckerman phantom represents the human form and its internal organs by using the mathematical equations of standard geometric shapes. It incorporates the major organs used in International Commission on Radiological Protection (ICRP) whole body dose calculations. It was revised in 1996 to include an esophagus and a neck section [7] and these revisions to the phantom were included in our modeling. In this study, the phantom was only used to estimate the absorbed dose to the red bone marrow and to provide an appropriate scatterer for returning neutrons to the head by reflection. Consequently (with the exception of the head) the lungs, skeletal system, and the body remainder were the only three tissue types included in the phantom. The compositions for these three tissues were taken from the Cristy/Eckerman 1987 report.

The phantom represents a male with height 1.74 m and a proportionate mass of 70 kg. Figure 3 is an anterior oblique view of the Cristy/Eckerman phantom. Note that the lungs are included in the skeletal image.

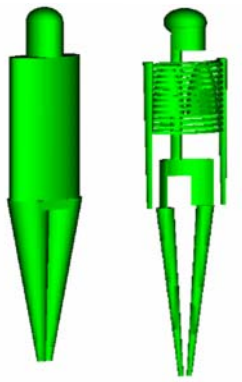

Figure 3. Anterior oblique view of the Cristy/Eckerman phantom and phantom skeleton

4 METHODS

4.1 Model Geometry

As shown in Fig. 4, for the moderator assembly calculations, the phantom was positioned such that the centerline of the moderator assembly was collinear with the centerline of the head phantom, and such that the top of the head was aligned with the downstream surface of the delimiter. Due to the lattice entry format for our implementation of the Zubal phantom, the details of that phantom are contained within the rectangular parallelepiped that is shown in the figure. For the INS calculation, the phantom was positioned such that the centerline of the circular INS source was collinear with the centerline of the head phantom. The neutrons were directed such that they were perpendicularly incident on the upstream surface of the rectangular parallelepiped (i.e., the top of the patient's skull.)

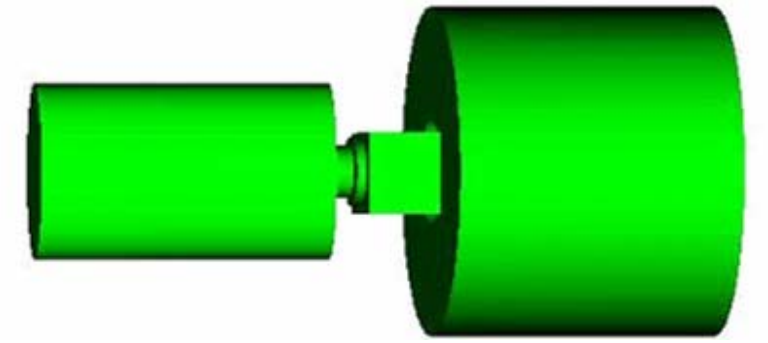

Figure 4. Patient orientation with respect to the moderator assembly

4.2 Absorbed Dose Calculations

In this study the neutron and gamma-ray absorbed doses to each structure in the Zubal phantom, and to each bone marrow region in the MIRD phantom, were calculated, on a per source neutron basis in MCNP, according to the equation

$$D'_j = \int k(E)\Phi p(E)dE \ , \tag{2}$$

where D_j is defined as the absorbed dose to structure or region j, k(E) is the particle kerma factor as a function of energy, and $\Phi_p(E)$ is the particle flux per source neutron as a function of energy.

4.3 Source Neutrons for Tolerance

In radiation therapy, the dose delivered to a tumor is limited by the tolerance of normal tissues which, because they are near the tumor or are in the path of the radiation, are also irradiated. The tumor dose is escalated until a normal tissue reaches some predetermined dose tolerance limit. For both calculating the effectiveness of the delimiter in shaping the radiation dose distribution within the patient's head, using the Zubal phantom, and for determining the effectiveness of the delimiter in reducing the patient's whole body radiation dose, using the

MIRD phantom, it is necessary to determine the number of source neutrons that corresponds to the tolerance of the normal tissues being reached. For the calculation of the radiation dose distribution within the patient's head we calculated the number of source neutrons that corresponds to the tolerance of the normal tissues being reached for the most dose limiting structure in the Zubal phantom. For the calculation of the patient whole body radiation dose with the MIRD phantom, we assumed that the same number of neutrons correspond to the tolerance limit.

We present below the mathematics for the calculation of the number of neutrons corresponding to the achievement of the tolerance dose. First of all, regarding notation, in this paper, we distinguish, with a prime, the absorbed doses per source neutron, from their unprimed counterparts (i.e. the neutron absorbed dose (D_n), the specific boron absorbed dose (d_B) and the photon absorbed dose (D_γ). The word specific, as used in the term, specific boron absorbed dose (d_B) means that the absorbed dose arising from neutron absorption reactions in boron is calculated for a ^{10}B concentration of one part per million (ppm) by weight. The specific boron absorbed dose (d_B) is distinguished from the boron absorbed dose (D_B) by using a lower case symbol.

The absorbed doses per source neutron were calculated for the structures within the Zubal phantom model using Eqn. 2 with the volume averaged flux calculated for each structure within the brain of the Zubal phantom using MCNP F4 tallies. Then we calculated for each structure, H_{RBE}, the low-LET radiobiogically equivalent (RBE) dose per source neutron for the mixed field of both high- and low- LET radiation resulting from BNCT treatment with a specified boron structure concentration. The RBE dose was calculated outside of the MCNP code using Eqn. 3:

$$H'_{RBE} = D'_\gamma + RBE_n \bullet D'_n + RBE_B CF \bullet Conc_B \bullet d'_B \ , \tag{3}$$

where RBE_n is the neutron RBE, $RBE_B CF$ is the product of the RBE and the compound factor (CF) for the boron absorbed dose, and $Conc_B$ is the concentration of ^{10}B (in ppm).

The values of the capture agent dependent coefficients that were used in the dose calculations are as follows: $RBE_B CF$ = 1.35, $Conc_B$ = 15 ppm, and $R_{t/b}$ =3.5, where $R_{t/b}$ (used in Eqn. 7) is the ratio of the ^{10}B concentration in the tumor to the ^{10}B concentration in the blood. The number of source neutrons (N) was determined such that the maximum structure RBE dose (among the many structures) equals the limiting RBE dose (H^{Tol}_{RBE}) for our calculations, which was assumed to be (12.8 Gy-Eq). Then,

$$N = \frac{12.8}{\max(H'_{RBE})} . \tag{4}$$

The treatment time (TT) was calculated using Eqn. 5

$$TT = N / n \ \ , \tag{5}$$

where n is the neutron source rate that is produced in the Li target.

4.4 Absorbed Dose Calculations to Brain Tissues

With a knowledge of N for the maximally exposed structure, the RBE doses for the less exposed structures were calculated as:

$$H_{RBE} = N \bullet H'_{RBE} \ . \tag{6}$$

Similarly, the high-LET tumor absorbed dose (D_T) henceforth called the 'tumor dose', was calculated, according to Eqn. 7 based on the number of neutrons, N, determined in Eqn. 4 as,

$$D_T = (D'_n + d'_B \bullet Conc_B \bullet R_{t/b}) \bullet N \ . \tag{7}$$

4.5 Objective Function

In order to assess the effectiveness of the delimiter in shaping the radiation dose distribution within the patient's head, we defined a new neutron field assessment parameter (NFAP). This new NFAP was developed to evaluate the complex dose distributions resulting from the mixed neutron and gamma ray fields that arise in the head of an individual who is treated for a malignant brain tumor using BNCT. The modified Zubal phantom was used to calculate the absorbed doses of different structures in the brain as well as the tumor dose. The new NFAP is based on absorbed dose distributions for normal structures and tumor, and yields a score that accounts for the competing goals of (1) sparing normal tissues and (2) maximizing tumor dose. It was formulated by modifying a previously defined Objective Function (OF), so that it is appropriate for BNCT. The resulting BNCT Objective Function (BOF) allows for the inclusion of tissue specific Relative Biological Effectiveness (RBE), and tissue specific dose tolerances and weights.

The BOF used here is an x-ray radiotherapy OF, modified to be appropriate for BNCT. The resulting BOF is the sum of two terms, as in Eqn. 8,

$$F = T + wC \,, \tag{8}$$

a tumor term (T) and a normal tissue term (C). A weighting factor (w) is included in the definition of F in order to allow the user to adjust the degree to which objective 1 is achieved in preference to the achievement of objective 2. The tumor term T is expressed as:

$$T = \frac{(D_T - D_T^{ref})\left|D_T - D_T^{ref}\right|}{(0.05 D_T^{ref})^2} \,, \tag{9}$$

where D_T is the high Linear Energy Transfer (LET) absorbed dose to the tumor and D_T^{ref} is a reference value of D_T. In the calculations presented herein, D_T^{ref} was set equal to 14.2Gy.

The mathematical form of the normal tissue term C is given by Eqns. 10 and 11, as

$$C = \sum_{i=1}^{N} C_i \ , \tag{10}$$

where

$$C_i = w_i \frac{\left(H_i - H_i^{tol}\right)^2}{\left(0.05 H_i^{tol}\right)^2} \ , \tag{11}$$

where H_i is the calculated RBE dose to the i_{th} normal tissue structure, H_i^{tol} is the tolerance dose for that structure and w_i is the relative importance weight for the i_{th} structure. In our calculations, all the normal tissue structures have been assigned the same weighting factor, $w_i = 1/M$, where M is the total number of normal tissues and all structures have been assigned the same tolerance dose $H_i^{tol} = H^{tol}$ =12.8 Gy-Eq.

4.6 Bone Marrow Dose

In BNCT, the absorbed dose to an organ is largely dependent on the concentration of the boron-containing compound within that organ. The concentration of boron in red bone marrow is not well known, but it is believed to be low enough that it can be ignored in calculation of the absorbed dose. For this reason, the red bone marrow absorbed dose, in the absence of boron, is used to assess the degree of patient protection provided by the moderator assembly delimiter. The kerma factors for red bone marrow listed in the International Commission on Radiological Units (ICRU) publication 46 [8] were used in this work for the calculations of absorbed dose to the red bone marrow. The absorbed dose in the red bone marrow, per source neutron was tallied, in MCNP, for the entire bone marrow volume in the MIRD phantom. The absorbed dose in the red bone marrow was calculated by multiplying the absorbed dose per source neutron by the number of source neutrons (N) from Eqn. 4.

$$D_{RM} = D'_{RM} \bullet N \ . \tag{12}$$

5 RESULTS

5.1 Effect of INS Beam Diameter

The results for the evaluation of beam size for the INS are presented below. Figure 5.1 is a graph of F versus INS beam diameter with the weighting function w as a parameter. Figure 5.1 shows that for small w, increasing the beam diameter leads to large F. For large w, F assumes a maximum for intermediately sized beam diameters. It should be noted that it is not appropriate to compare among curves of different w, since curves with larger w will necessarily have larger objective function scores due to the linear dependence of F on w given in Eqn. 8.

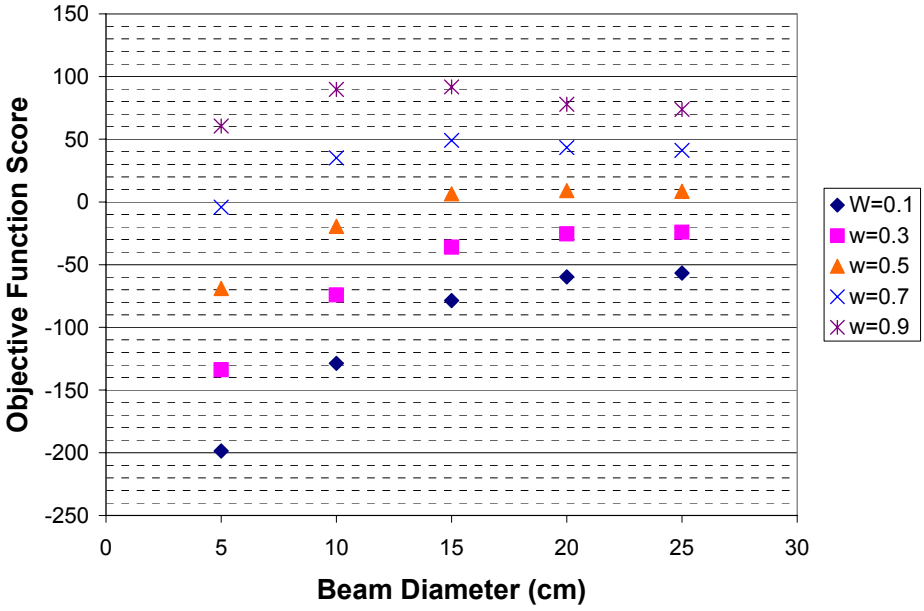

Figure 5.1. Objective Function score for various INS beam diameters and 5 weighting factors

Figure 5.2 is a graph of the absorbed dose to bone marrow (D_{RM}) versus INS beam diameter. Figure 5.2 shows that increasing the beam diameter leads to larger D_{RM}.

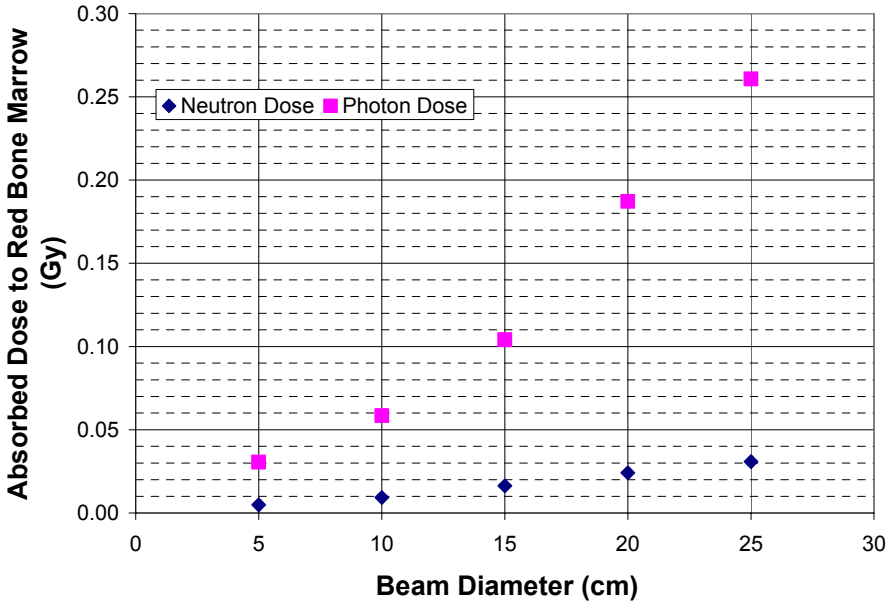

Figure 5.2. Absorbed dose to red bone marrow for various INS beam diameters

Figure 5.3 is a graph of F versus the treatment port diameter, with the weighting factor w as a parameter, for the moderator assembly for a delimiter thickness of 11cm. Figure 5.3 shows that, unlike for the INS, for the moderator assembly, increasing the treatment port diameter leads to smaller F, for w=0.1 and treatment port diameters less than 25cm. For larger w, the shapes of the curves of F versus treatment port diameter are very similar to the shapes of the corresponding curves for the INS. For w=0.9, for both the INS and the moderator assembly, F assumes a maximum value of approximately 100 for diameters of 15cm.

Figure 5.4 is a graph of D_{RM} versus the moderator assembly treatment port diameter for a delimiter thickness of 11cm. Figure 5.4 shows that increasing the diameter of the moderator assembly treatment port leads to smaller gamma-ray D_{RM} and only small non-monotonic variations in the neutron D_{RM}.

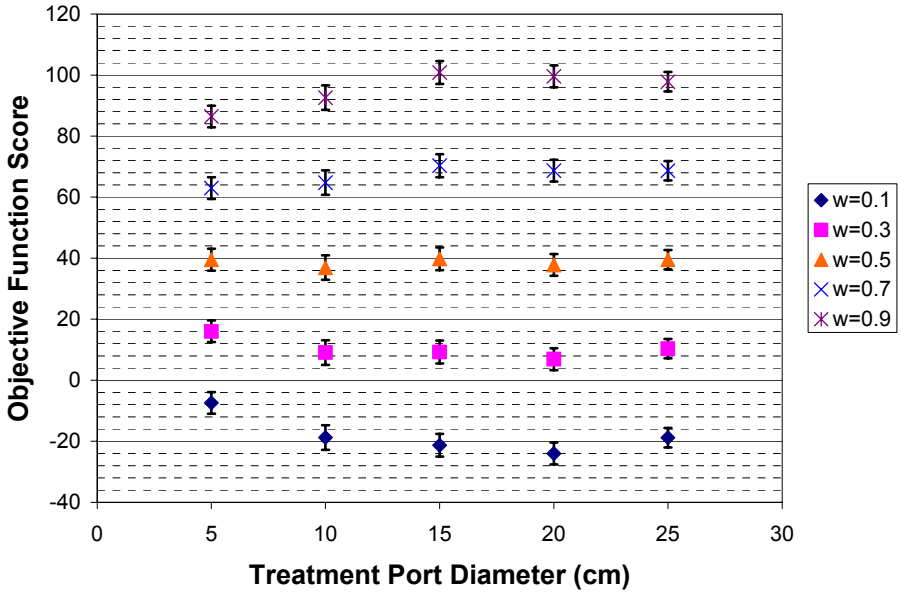

Figure 5.3. Objective Function score for various treatment port diameters and 5 weighting factors for a delimiter thickness of 11cm

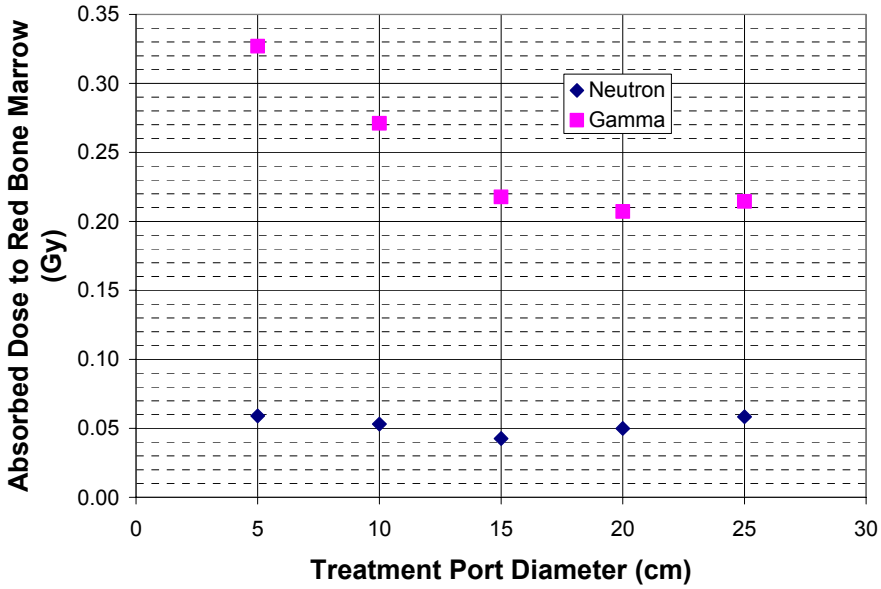

Figure 5.4. Absorbed dose to red bone marrow for various treatment port diameters

Figure 5.5 is a graph of F versus moderator assembly delimiter thickness, with the weighting factor w as a parameter, for a treatment port diameter of 25cm. For small values of w, increasing the delimiter thickness leads to slightly smaller F. For large values of w, increasing the delimiter thickness causes almost no change in F.

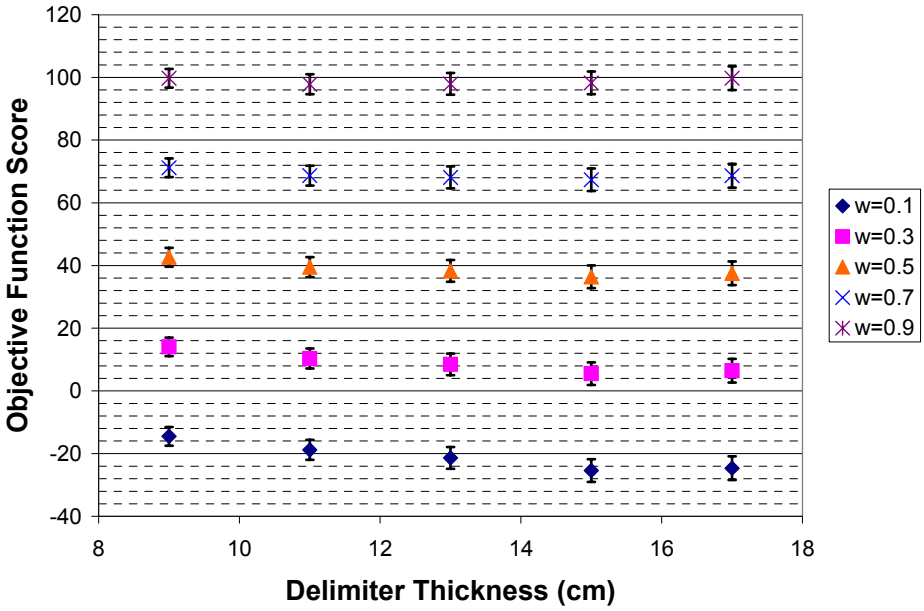

Figure 5.5. Objective Function scores for various delimiter thicknesses and 5 weighting factors for a treatment port diameter of 25cm

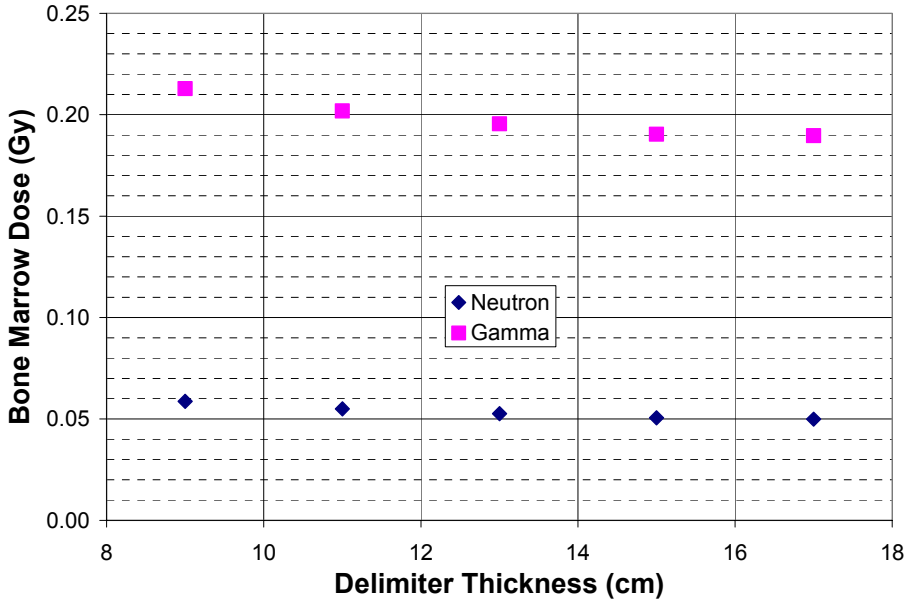

Figure 5.6. Absorbed dose to red bone marrow for various delimiter thicknesses, for a treatment port diameter of 25cm

Figure 5.6 is a companion graph to Fig. 5.5. Figure 5.6 is a graph of D_{RM} versus moderator assembly delimiter thickness with the weighting function w as a parameter for a treatment port diameter of 25cm. Figure 5.6 shows that, for a 25cm diameter treatment port, increasing the thickness of the delimiter decreases both the gamma-ray and the neutron D_{RM}.

6 CONCLUSION

As part of an effort to design a moderator assembly for an ABNS for BNCT, we have implemented a modified version of the Zubal Phantom (a voxel-based head phantom that delineates detailed structures inside the brain) in MCNP5. As the component of the moderator assembly that is closest to the patient, the shape and material of the delimiter is important to the quality of the neutron beam. Using our Zubal Phantom MCNP model, we have evaluated various moderator assembly delimiter designs. The evaluation was based on the calculation of a new neutron field assessment parameter (NFAP) that we developed to evaluate the complex dose distributions resulting from the mixed neutron and gamma-ray fields that arise in the head of an individual who is treated for a malignant brain tumor using BNCT. The modified Zubal phantom was used to calculate the absorbed doses of different structures in the brain as well as the tumor dose. The new NFAP is based on absorbed dose distributions for normal tissue structures and tumor, and yields a score that accounts for the competing goals of sparing normal tissues and maximizing tumor dose. It was formulated by modifying a previously defined Objective Function, so that it is appropriate for BNCT. In addition to assessing the effect of the delimiter on the BOF, this paper assesses the effect of the delimiter in reducing the whole body dose to the bone marrow using MCNP with a MIRD whole body phantom.

Both sets of calculations were performed for two modeled sources. One modeled source is based on a recent iteration of the OSU ABNS design. The other modeled source represents an idealized neutron source (INS) for BNCT that is perpendicularly incident and perfectly collimated with a 1/E neutron energy spectrum within appropriate energy limits. The latter source was modeled to serve as an easily reproducible benchmark source, for the verification of our results by others and to help us recognize appropriate delimiter behavior in our calculations for the OSU ABNS design.

For the INS the dependence of the BOF on the beam diameter is easily understood. If having a larger tumor dose is valued highly, then the beam diameter should be made large. If on the other hand protecting normal tissues is valued highly, then the beam diameter should be made of intermediate size. In either case, increasing the beam diameter increases the gamma-ray and neutron red bone marrow absorbed dose.

The behavior for the ABNS moderator assembly is observed to be far from ideal. For example, for small normal tissue weighting factors, w, graphs of the BOF versus treatment port diameter are differently shaped than graphs of the BOF versus INS beam diameter. Also, decreasing the treatment port diameter causes the red bone marrow absorbed dose (D_{RM}) to increase (a behavior that is also contrary to that for the INS). However the dependence of D_{RM} on delimiter thickness is as one would expect, showing greater protection of the red bone marrow with greater delimiter thickness.

7 REFERENCES

1. M. Cristy and K.F. Eckerman, "Specific Absorbed Fractions of Energy at Various Ages from Internal Photon Sources. I. Methods," *Oak Ridge National Laboratory,* **ORNL/TM-8381/V1** (1987).
2. G.I. Locher, *Am. J. Roetgenol* **36:1,** (1936).
3. J.W. Blue, W.K. Roberts, T.E. Blue, R.A. Gahbauer and J.S. Vincent "A Study of Low Energy Proton Accelerators for Neutron Capture Therapy," *Neutron Capture Therapy,* H. Hatanaka, ed., Nishimura Niigata, (1986).
4. M.C. Dobelbower, *An Integrated Design of an Accelerator-Based Neutron Source for Boron Neutron Capture Therapy,* The Ohio State University, Dissertation, (1987).
5. I.G. Zubal, C.R. Harrel, E.O. Smith and A.L. Smith, "Two dedicated software voxel-based, anthropomorphic (torso and head) phantoms," *Proceedings of the International Workshop,* National Radiological Protection Board, Chilton, UK, on 6 and 7 July 1995, pp.105-111 (1996).
6. J.F. Evans, T.E. Blue and N. Gupta, "Absorbed dose estimates to structures of the brain and head using a high-resolution voxel-based head phantom," *Med. Phys.* **28(5)**, pp.780-786, (2001).
7. "The ORNL mathematical phantom series," http://homer.ornl.gov/vlab/mird2.pdf (1996)
8. International Commission on Radiation Units and Measurements, "Photon Electron, Proton and Neutron Interaction Data for Body Tissues," ICRU Report 46, (1992).